Title
DECK MODEL FOR TRIPLE-REGGE COUPLINGS

Author
Sorensen, Cristian.

Publication Date
1972-04-24

Submitted to Physical Review

LBL-908
Preprint c.1

DECK MODEL FOR TRIPLE-REGGE COUPLINGS

Cristian Sorensen

April 24, 1972

AEC Contract No. W-7405-eng-48

DECK MODEL FOR TRIPLE-REGGE COUPLINGS*

Cristian Sorensen

Lawrence Berkeley Laboratory
University of California
Berkeley, California 94720

April 24, 1972

ABSTRACT

Inclusive cross sections in the triple-Regge region are calculated using a version of the ABFST multiperipheral model that amounts to an extension of the Deck model. Even though almost no parameters are available for adjustment, presently available moderate-energy data are described in a qualitatively satisfactory manner. Predictions are made for future experiments at higher energies, and the various triple-Regge couplings are extracted from the model. It is found that vertices corresponding to high-lying trajectories are suppressed. In particular the dimensionless parameter η_{PPP} that characterizes the triple-Pomeranchon vertex turns out to be $\lesssim 10^{-3}$.

I. INTRODUCTION

The new generation of accelerators will explore the region of phase space where a triple-Regge expansion[1] is expected to be useful. It is, therefore, of interest to advance theoretical estimates concerning the magnitudes of cross sections, the reliability of a triple-Regge expansion and the relative strengths of the various triple-Regge couplings.[1] This last point is especially important if one is interested in resolving a specific vertex like, say, the triple-Pomeranchon.

Triple-Regge formulas have been known for some time to researchers investigating multi-Regge models.[2] It, therefore, seems natural to use a specific and reasonably realistic multiperipheral model to deal with the questions raised above.

We have employed a modified ABFST model[3,4] to attempt an answer. It will be apparent later that, in this particular application, our multiperipheral model amounts to an extended Deck model.[7] To gain some confidence in it, we have also calculated inclusive distributions at presently accessible accelerator energies and obtained satisfactory results.[8]

The remaining sections are organized as follows: Section II describes the model, including some of the technical details; Section III presents the results at moderate and high energies; Section IV discusses some of the properties of the triple-Regge vertices in this model; and Section V attempts to summarize the results and draw conclusions.

II. THE MODEL

We are interested in calculating the double-differential cross section $(d^2\sigma)/(ds'd|t|)$ for the inclusive experiment

$$a + b \rightarrow c + X ,$$

where

$$s' = (p_a + p_b - p_c)^2 ,$$

$$t = (p_a - p_c)^2 ;$$

we also define

$$s = (p_a + p_b)^2 .$$

The inclusive cross section may be obtained by summing over the exclusive ones. For the latter, we use a multiperipheral model of the type discussed in Ref. 3 and schematically represented in Fig. 1. Since we are interested in the region where $s/s' \gg 1$ and $t/s \ll 1$, we allow the scattering represented by the leftmost blob of Fig. 1 to take place at high energies as well as low.[4]

As explained in Refs. 3 and 5 multiperipheral models yield a very simple result for the one particle inclusive cross section

$$\frac{d^2\sigma}{ds'd|t|} = \frac{\sum_i}{2\lambda^{\frac{1}{2}}(s,m_a^2,m_b^2)} \int ds_3\ dp_c\ dk\ d^4K\ \delta(K^2 - s_3)$$

$$\times\ 2\lambda^{\frac{1}{2}}(s_3,\mu_\pi^2,m_b^2)\ \sigma^{TOTAL}_{\pi_i b}(s_3)\ \frac{|A\pi_i a \rightarrow \pi_i c(s_1,t)|^2}{(\mu_\pi^2 - u)^2}$$

$$\times\ \delta(t' - t)\ \delta(s' - s'')\ \delta^4(p_a + p_b - p_c - k - K) \qquad (1)$$

$\sum_i$ indicates a sum over the three charge states of the pion,

$$dp_c = \frac{d^3p_c}{2(p_c^2 + m_c^2)^{\frac{1}{2}}}\ \frac{1}{(2\pi)^3} \quad \text{and similarly for} \quad dk$$

$$s_1 = (p_c + k)^2$$

$$t' = (p_a - p_c)^2$$

$$u = (p_a - p_c - k)^2$$

$$s'' = (p_a + p_b - p_c)^2$$

$$\lambda(x,y,z) = x^2 + y^2 + z^2 - 2xy - 2xz - 2yz.$$

Formula (1) is represented schematically in Fig. 2. Depending on the quantum numbers of particles a, b, and c, it may also be necessary to add contributions like the ones shown in Fig. 3. In our calculation of $p + p \rightarrow p + X$ (see Sec. III), such terms have to be included.

The reader will recognize in Fig. 2 an extended Deck model.[7] In previous applications of such a model the total cross section on the right was restricted to a given resonance (e.g., Δ or ρ), in our case we use the total cross section for any energy.

The detailed structure of the multiperipheral chain is never used. The only feature required is the capacity for generating a realistic total cross section. The details could be much more complicated than the simple model of Ref. 3.

If the limit $s' \rightarrow \infty$, $s/s' \rightarrow \infty$ is taken, one obtains,[10] assuming that high-energy scattering is well described by Regge poles:

$$\frac{d^2\sigma}{ds'\,d|t|} = \frac{1}{16\pi s^2} \sum_{i,j,k} \beta_{a\bar{c}i}(t)\, \beta_{\bar{a}cj}(t)\, \zeta_i(t)\, \zeta_j^*(t)$$

$$\times \left(\frac{s}{s'}\right)^{\alpha_i(t)+\alpha_j(t)} s'^{\alpha_k(0)}\, g_{ij,k}(t)\, \beta_{b\bar{b}k}(0) \qquad (2)$$

where

$$g_{ij,k}(t) = \frac{3}{16\pi^3} \int_{-\infty}^{0} \frac{du}{(\mu_\pi^2 - u)^2} \left[\lambda^{\frac{1}{2}}(\mu_\pi^2,u,t)\right]^{\alpha_i(t)+\alpha_j(t)}$$

$$\times\ \beta_{\pi\pi i}(\mu_\pi^2,u,t)\, \beta_{\pi\pi j}(\mu_\pi^2,u,t)\, \beta_{\pi\pi k}(u,u,0) \cdot \int_0^{(u/t)^{\frac{1}{2}}e^{-q}} dx\, x^{\alpha_k(0)}$$

$$\times\ P_{\alpha_i(t)+\alpha_j(t)}(z)\ ; \qquad (3)$$

$$z = \frac{\operatorname{ch} q - (t/u)^{\frac{1}{2}}\, x}{\operatorname{sh} q} \qquad \operatorname{ch} q = \frac{\mu_\pi^2 - u - t}{2(ut)^{\frac{1}{2}}}\ ;$$

β denotes a factorized Regge residue, ζ a signature factor. In formula (3), the fact that one of the pion masses is not μ_π^2 has been exhibited explicitly. We will have more to say about this later.

The normalization of the residues is such that the contributions of a pole i to the (a,b) total cross section and to the elastic differential cross section are:

$$\sigma^{\text{Total}}_{i,ab}(s) = \frac{1}{\lambda^{\frac{1}{2}}(s,m_a^2,m_b^2)}\, \beta_{a\bar{a}i}(0)\, \beta_{b\bar{b}i}(0)\, s^{\alpha_i(0)}$$

$$\frac{d\sigma_{i,ab}(s,t)}{dt} = \frac{1}{16\pi\lambda(s,m_a^2,m_b^2)}\, |\beta_{aai}(t)\, \beta_{bbi}(t)\, \zeta_i(t)|^2 .$$

The factor 3 in formula (3) reflects the three charge states of the pion. It is correct if the trajectories i and j have the quantum numbers of the vacuum.[16]

In our calculation of $p + p \to p + X$ by means of formula (1), we have used the experimentally observed (π,p) total cross sections together with isospin invariance. For the elastic amplitude $A_{\pi N\to\pi N}$, we have adopted the following simplifying prescription, $A_{\pi N\to\pi N}(s,t) = A_{\pi N\to\pi N}(s,0)\, e^{\gamma t}$. This form is fairly accurate for small t, even in the resonance region, when γ is taken to be $\approx 4(\text{GeV/c})^{-2}$. For $A_{\pi N\to\pi N}(s,0)$ we used the tabulation of Ref. 17.

Off-shell corrections to the πN elastic amplitude and πN total cross section have been introduced to provide the necessary cut-off in the integrals over the virtual pion mass. We have used a form factor of the type suggested by the ABFST integral equation:[3]

$$A_{\pi N}(s,t,u) = A_{\pi N}(s,t,u=\mu_\pi^2) \left[\frac{u_0}{u_0 - \frac{1}{2}(\mu_\pi^2 + u - \frac{t}{2})}\right]^{(\bar{\alpha}+1)}$$

$$\sigma_{\pi N}(s,u) = \sigma_{\pi N}(s,u=\mu_\pi^2) \left[\frac{u_0}{u_0 - u}\right]^{\bar{\alpha}+1} .$$

The ABFST model suggests that the asymptotic behavior of the residue β_i of the pole i is $(-u)^{\alpha_i+1}$ as $-u \to \infty$. Since, for low energies, we do not use a Regge parametrization of σ_{Total} or of $A_{\pi N \to \pi N}$, we cannot incorporate this result in a simple manner. Motivated by the perturbative approach of Refs. (4) and (10) we have taken an average intercept $\bar{\alpha} = 0.7$.

The form of the off-shell corrections given above has been shown to provide an adequate fit to numerical solutions of the ABFST equation even in the low-virtual-mass region if $u_0 \approx 1$ GeV^2.[15] We have experimented with other cutoff procedures, such as "reggeizing" the pion, and found that the results do not change significantly. Thus our model contains almost no free parameters.

III. RESULTS AT INTERMEDIATE AND HIGH ENERGIES

Figure 4 shows a comparison of the predictions of the model for the process $pp \to pX$ with the experimental results of Anderson et al.[6] The following aspects of the experimental data are satisfactorily reproduced:

(i) Energy dependence: one of the striking features of the data of Ref. 6 is a rapid decrease of the average cross section with increasing beam momentum. This effect, indicative of the weakness of diffractive excitation in this energy range, is well reproduced by the model.

(ii) Missing mass dependence: Given that we cannot expect to reproduce the full resonance structure, we consider our results satisfactory. The calculations yield bumps in the missing mass at the appropriate locations[11] but with insufficient strength.

(iii) Absolute normalization: This point is sensitive to the cutoff procedure adopted for the integration over the momentum transfer u in formulas (1) and (2). This is the problem of off mass-shell corrections mentioned in Sec. II. It may be seen from Fig. 4 that our normalization is better for high missing masses, where resonances are not expected to be important.

Another interesting result from our calculations is the importance, at intermediate energies and small t, of pion exchange, in the sense of Fig. 3b. For high missing masses, this mechanism accounts for about 50% of the cross section at $p_{lab} = 20$ GeV/c and $t \approx -0.04$ (GeV/c)^2. The importance of diagram 3b has also been recognized recently by other authors.[8,9]

Figure 5 exhibits the t dependence of the double differential cross section for a fixed value of the incident energy, at various values of the missing mass. Comparison with the data is again satisfactory.

The broken curve in Fig. 4 shows that a triple Regge expansion with the vertices predicted by the model (see Table I) provides a reasonably accurate approximation to the more exact calculation even at low energies.[19]

Figure 6 shows what we expect to observe at higher energies on the basis of this model. Dominance of the triple-Pomeranchon component would give a flat, energy-independent, curve in Fig. 6. The broken line at the bottom of the graph is what $g_{PP,P}$ alone contributes to the double differential cross section. It can be seen that, for the ISR energies, this contribution can amount to about 50% of the cross section in the appropriate missing mass range ($s' \sim 10\text{-}30\ \mathrm{GeV}^2$). Thus it may be possible to extract the value of $g_{PP,P}$ by means of a fit to the data.

Figure 7 shows a comparison of the recent results of the CERN-IHEP boson spectrometer[18] (continuous curve) with a triple-Regge expansion with the vertices predicted by our model. It can be seen that our expansion yields a very satisfactory missing mass dependence and energy dependence.

IV. TRIPLE-REGGE VERTICES

Table I exhibits the values of the various triple-Regge vertices as predicted by our model. Not that the $g_{ij,k}$ are not dimensionless. The values we give are to be used in an expansion like formula (2), where the energy scale parameter is $1\ \mathrm{GeV}^2$.

According to Table I, all the couplings are of the same order of magnitude. There is, however, a definite trend. The higher the intercept of trajectories i and j, the smaller the coupling.

The rough equality of the vertices derives, in this model, from the comparable values of the couplings of the P and the P' to the $\pi\pi$ system, as extracted from total cross sections. The relation between the strength of the vertex and the height of the intercept can be understood most easily by writing formula (3) for $t = 0$

$$g_{ij,k}(0) \propto \frac{1}{16\pi^3} \frac{3}{\alpha_k(0)+1} \int_{-\infty}^{0} du(\mu_\pi^2 - u)^{\alpha_i(0)+\alpha_j(0)-2-\alpha_k(0)}$$

$$\times\ (-u)^{\alpha_k(0)+1}\ \beta_{\pi\pi i}(u,\mu_\pi^2,0)\ \beta_{\pi\pi j}(u,\mu_\pi^2,0)\ \beta_{\pi\pi k}(u,u,0) \qquad (4)$$

or, letting $\mu^2 \approx 0$,

$$g_{ij,k}(0) \propto \frac{1}{16\pi^3} \frac{3}{\alpha_k(0)+1} \int_{-\infty}^{0} du(-u)^{\alpha_i(0)+\alpha_j(0)-1}$$

$$\times\ \beta_{\pi\pi i}(0,0,0)\ \beta_{\pi\pi j}(0,0,0)\ \beta_{\pi\pi k}(0,0,0) \left(\frac{u_0}{u_0 - \frac{u}{2}}\right)^{\alpha_i(0)+\alpha_j(0)+2}$$

$$\times \left(\frac{u_0}{u_0 - u}\right)^{\alpha_k(0)+1} . \qquad (4')$$

In (4') we have exhibited the explicit form of the off-shell corrections.

The influence both of the trajectory intercept and of the magnitude of the couplings of the trajectories to the $\pi\pi$ system is exhibited in (4) and (4'). Note that we use the appropriate values for the trajectory intercepts in the form factors. Since we have singled out a specific set of trajectories we do not have to use an average intercept as we did in Sec. II.

The effect of the trajectory intercept can be traced back to kinematical limitations on the minimum momentum transfer u between the two blobs of Fig. 3 when s_1 and s_3 are large.

The reader may have noticed that the only secondary trajectory included in Table I is the P'. As already discussed in footnote 16, the ρ and A_2 trajectories are not important for the $p + p \rightarrow p + X$ and $\pi p \rightarrow X + p$ experiments in the kinematical regions that we have been considering. However, the absence of the ω coupling is more serious. So long as we restrict ourselves to π exchange, the ω decouples. This circumstance can be interpreted either as an interesting consequence of the π-exchange model or as a disturbing

violation of the cherished, and empirically well supported, notion of exchange degeneracy. Note that, if degeneracy is assumed, the extraction of $g_{PP,P}$ from experimental fits becomes easier because nondiagonal terms of the form (PP',k) are approximately cancelled by terms with P' replaced by ω.

V. CONCLUSIONS

The existence of the pion pole in connected parts together with the pole factorization theorem implies that the triple-Pomeranchon vertex cannot vanish.[20] The question is then whether the contribution to the cross section from the region of phase space dominated by the pion pole is a significant fraction of the total. We believe that the results of Sec. III show that the pion pole has something to do with the observed cross sections. We have not attempted to fit the data but rather to show that the gross features could be reproduced with a very simple model. Section IV, however, shows that the triple-Pomeranchon vertex is so small as to be almost unobservable except at extremely high energies.

The dimensionless parameter[10] η_{PPP} that determines the displacement of $\alpha_P(0)$ from 1 is, assuming $\alpha_P' = 0.5\ (\mathrm{GeV/c})^{-2}$

$$\eta_{PPP} = \frac{g^2_{PP,P}(0)}{16\pi\ 2\alpha_P'(0)} \approx 5 \times 10^{-4}.$$ [12]

ACKNOWLEDGMENTS

I am grateful to Mordechai Bishari, Chun Fai Chan, Geoffrey Chew, and Martin Einhorn for many valuable discussions. Professor Chew suggested this investigation and provided indispensable guidance and advice.

FOOTNOTES AND REFERENCES

* This work was supported by the U. S. Atomic Energy Commission.

1. C. E. DeTar et al., Phys. Rev. Letters 26, 675 (1971).
2. For a survey of the early literature see R. D. Peccei and A. Pignotti, Phys. Rev. Letters 26, 1076 (1971).
3. D. Amati, A. Stanghellini, and S. Fubini, Nuovo Cimento 26, 896 (1972); L. Bertocchi, S. Fubini, and M. Tonin, Nuovo Cimento 25, 626 (1972).
4. G. F. Chew, T. Rogers, and D. R. Snider, Phys. Rev. D2, 765 (1970); G. F. Chew and D. R. Snider, Phys. Rev. D3, 420 (1971); G. F. Chew and D. R. Snider, Phys. Rev. D1, 3453 (1970).
5. S. Fubini, in Strong Interactions and High-Energy Physics, edited by R. G. Moorhouse (Plenum Press, New York, 1964).
6. E. W. Anderson et al., Phys. Rev. Letters 16, 855 (1966) and R. M. Edelstein et al., Isobar Production and Elastic Scattering in pp Interactions From 6-30 GeV/c, Carnegie-Mellon University report.
7. R. T. Deck, Phys. Rev. Letters 13, 169 (1964).
8. Successful calculations of inclusive cross sections from a multi-peripheral model have also been reported recently by F. Duimio and G. Marchesini, Phys. Letters 37B, 427 (1971).
9. M. Bishari, Phys. Letters 38B, 510 (1972).
10. H. D. I. Abarbanel et al., Phys. Rev. Letters 26, 675 (1971) and Princeton University report (April 1971) to be published in Ann. Phys. (New York).
11. Given the success of Deck models in describing diffractively produced resonances, this is not very surprising. For more details on this subject see Ref. 13.

12. The authors of Ref. 10 obtained a much bigger value because (i) They assumed exchange of the full pseudoscalar meson octet instead of just the π triplet. This gives in η_{PPP} an extra factor of $(8/3)^2 \sim 7$; (ii) They were working in a perturbative scheme in which $\alpha_\rho(0) \approx 0.7$. According to the discussion of Sec. IV this will make η_{PPP} larger; (iii) The $\pi\pi$ asymptotic total cross section then used was about a factor of 2 larger than what is expected from factorization. Given that $\eta_{PPP} \propto (\sigma_{\pi\pi}^{TOTAL})^3$ an additional factor ≈ 8 is introduced.
13. E. L. Berger, Phys. Rev. 179, 1567 (1969) and references therein.
14. V. D. Barger and D. B. Cline, Phenomenological Theories of High Energy Scattering (W. A. Benjamin Inc., New York, 1969).
15. C. F. Chan and B. R. Webber, Solution of the ABFST Equation with a Resonance Kernel, Lawrence Berkeley Laboratory Report LBL-341 September 1971, to be published in Phys. Rev. D. I am indebted to Chun Fai Chan for valuable discussions of this question.
16. We have in mind $p + p \to p + X$ experiments. The ρ and A_2 trajectories are known empirically to couple weakly to the $N\bar{N}$ system at small t. The ω does not couple to $\pi\pi$ due to G-parity conservation.
17. G. Höhler and R. Strauss, Tables of Pion-Nucleon Forward Amplitudes, University of Karlsruhe Report, October 1971.
18. Y. M. Antipov et al., Missing-mass Spectra Observed in $\pi^- p \to p + X^-$ at 25 and 40 GeV/c, February 1972 (submitted to Phys. Letters).
19. Since we were interested in the averaging properties of the triple-Regge expansion for low values of the missing mass, we

have used the variable $\nu = s' - m_b^2 - t$ instead of s' in formula (2). This is consistent with what is usually done when extrapolating asymptotic expansions for two-body reactions to low values of the energy. When $s' \gg m_b + t$ the variables coincide. I am indebted to Stephen Ellis and Tony Sanda for suggesting the use of this variable.

20. G. F. Chew, private communication, Lawrence Berkeley Laboratory, Summer 1971.

Table I. Triple-Regge vertices.[a]

t (GeV/c)^2	PP,P	PP',P	P'P',P	PP,P'	PP',P'	P'P',P'
0	0.142	0.299	0.745	0.236	0.488	1.21
-0.05	0.135	0.293	0.734	0.244	0.523	1.31
-0.10	0.127	0.285	0.734	0.247	0.547	1.40
-0.15	0.118	0.275	0.733	0.246	0.562	1.48
-0.20	0.109	0.263	0.731	0.240	0.569	1.55
-0.25	0.099	0.251	0.726	0.231	0.567	1.61
-0.30	0.091	0.237	0.719	0.219	0.559	1.65
-0.35	0.082	0.223	0.709	0.206	0.546	1.68

[a] Values of the triple-Regge vertices as a function of t, assuming that $\beta_P(t)$ varies as $e^{1.5t}$ and that $\beta_{P'}(t)$ is a constant. The magnitude of the coupling of the P to the $\pi\pi$ system has been obtained via factorization assuming that the asymptotic πN and $\pi\pi$ cross sections are 23 mb and 38 mb respectively. The P' was assumed to couple to the $\pi\pi$ system with the same strength as the P. This is empirically well supported (see for example, Ref. 14). The couplings given above are to be used with and expansion like Eq. (2). The scale parameter in the form factor has been taken to be $u_0 = 1$ GeV^2.

FIGURE CAPTIONS

Fig. 1. Schematic representation of the exclusive matrix element.

Fig. 2. Schematic representation of formula (1). If the detected particle is a pion other diagrams having a pion coming not from the leftmost blob may have to be considered. The contribution of these other terms is not important very close to the kinematical boundary.

Fig. 3. Other terms that may have to be included depending on the quantum numbers of particles a, b, and c.

Fig. 4. Comparison of our results with the data of Anderson et al. The diamonds (◇) correspond to the experimental values, the smooth curve is our calculation and the broken line is what a triple-Regge expansion with the couplings of Table I predicts. In 4 (a-d) we have plotted the same quantity as have the authors of Ref. 6 for "fixed" t and varying energy (see the relevant footnotes in Ref. 6).

Fig. 5. Comparison of our results with the t dependence of the data of Ref. 6 at three different values of the missing mass: (a), $(s')^{\frac{1}{2}} = 1.4$ GeV; (b), $(s')^{\frac{1}{2}} = 1.7$ GeV; (c), $(s')^{\frac{1}{2}} = 1.9$ GeV. The normalization of our results has been adjusted to coincide with the data at the lowest value of t.

Fig. 6. Expectations at higher energies. We plot $\ln[s'(d^2\sigma)/(ds'dt)]$ versus $\ln s'$ at $t = -0.04$ $(\mathrm{GeV}/c)^2$. The triple-Pomeranchon component, if sufficiently strong, would be evident as an almost flat, energy independent, section of the curve. The flat broken line at the bottom of the graph is the contribution of the triple Pomeron. The

curvature at small s' is due to the use of the variable $\nu = s' - m_b^2 - t$ instead of s'. See footnote 19. Continuous lines are the result of calculating with the complete model; broken lines correspond to the triple-Regge expansions. The reaction is $p + p \to p + X$.

Fig. 7. The experimental results of the CERN-IHEP boson missing-mass spectrometer (continuous curves) compared with the predictions of a triple-Regge expansion with the vertices given in Table I. We have taken $t = -0.25$ $(\mathrm{GeV}/c)^2$. The experimental $|t|$ varies between 0.17 $(\mathrm{GeV}/c)^2$ and 0.35 $(\mathrm{GeV}/c)^2$.

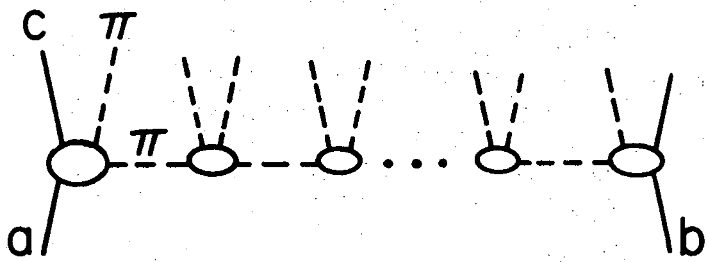

Fig. 1

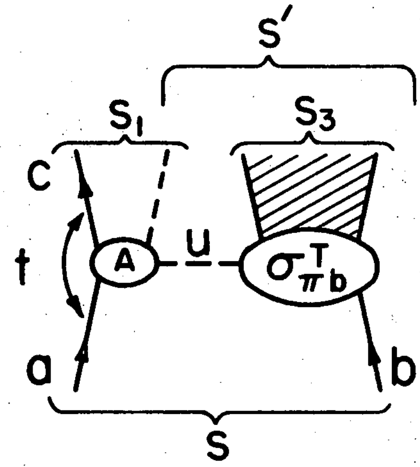

Fig. 2

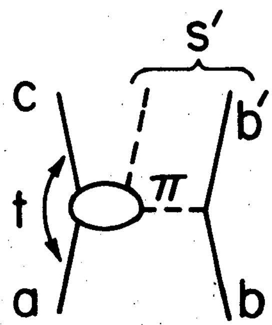

Fig. 3a

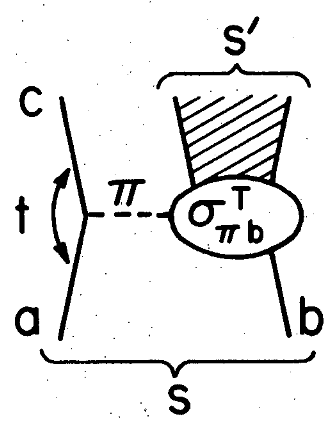

Fig. 3b

XBL724-2836

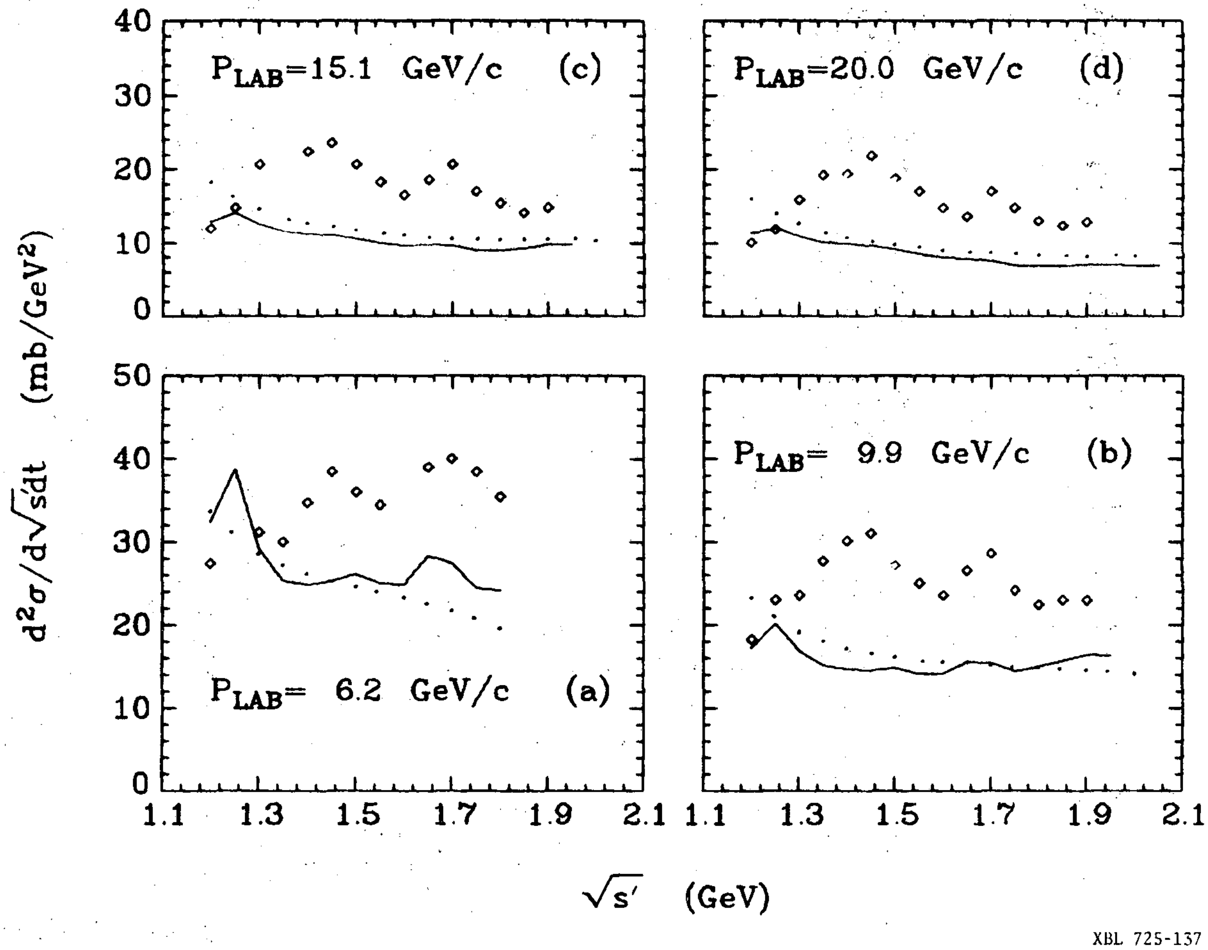
PLAB=15.1 GeV/c (c)
PLAB=20.0 GeV/c (d)
PLAB= 6.2 GeV/c (a)
PLAB= 9.9 GeV/c (b)
d2σ/d√s'dt (mb/GeV2)
√s' (GeV)
0
10
20
30
40
50
1.1
1.3
1.5
1.7
1.9
2.1
XBL 725-137

Fig. 4a - d

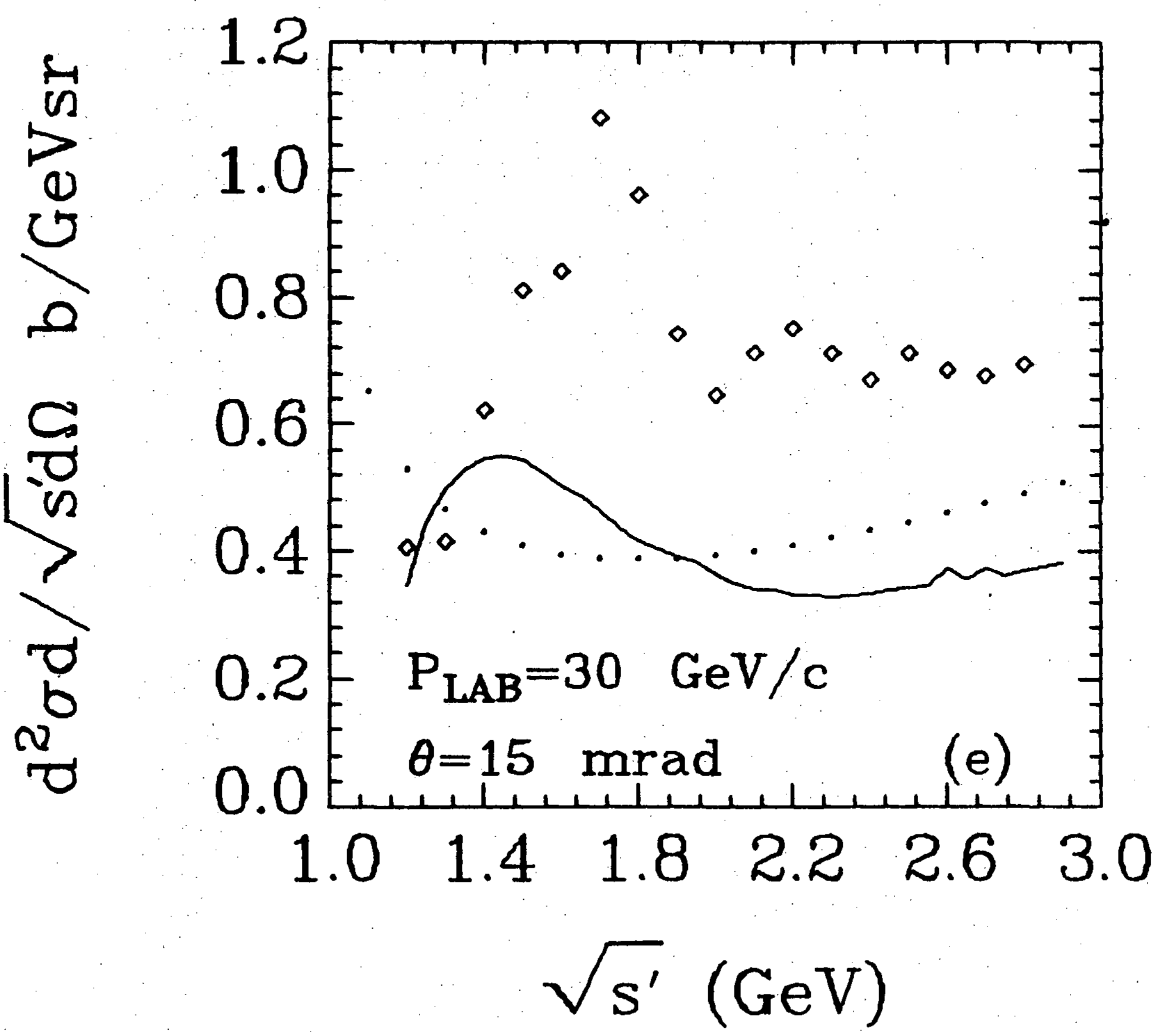

XBL 725-138

Fig. 4e

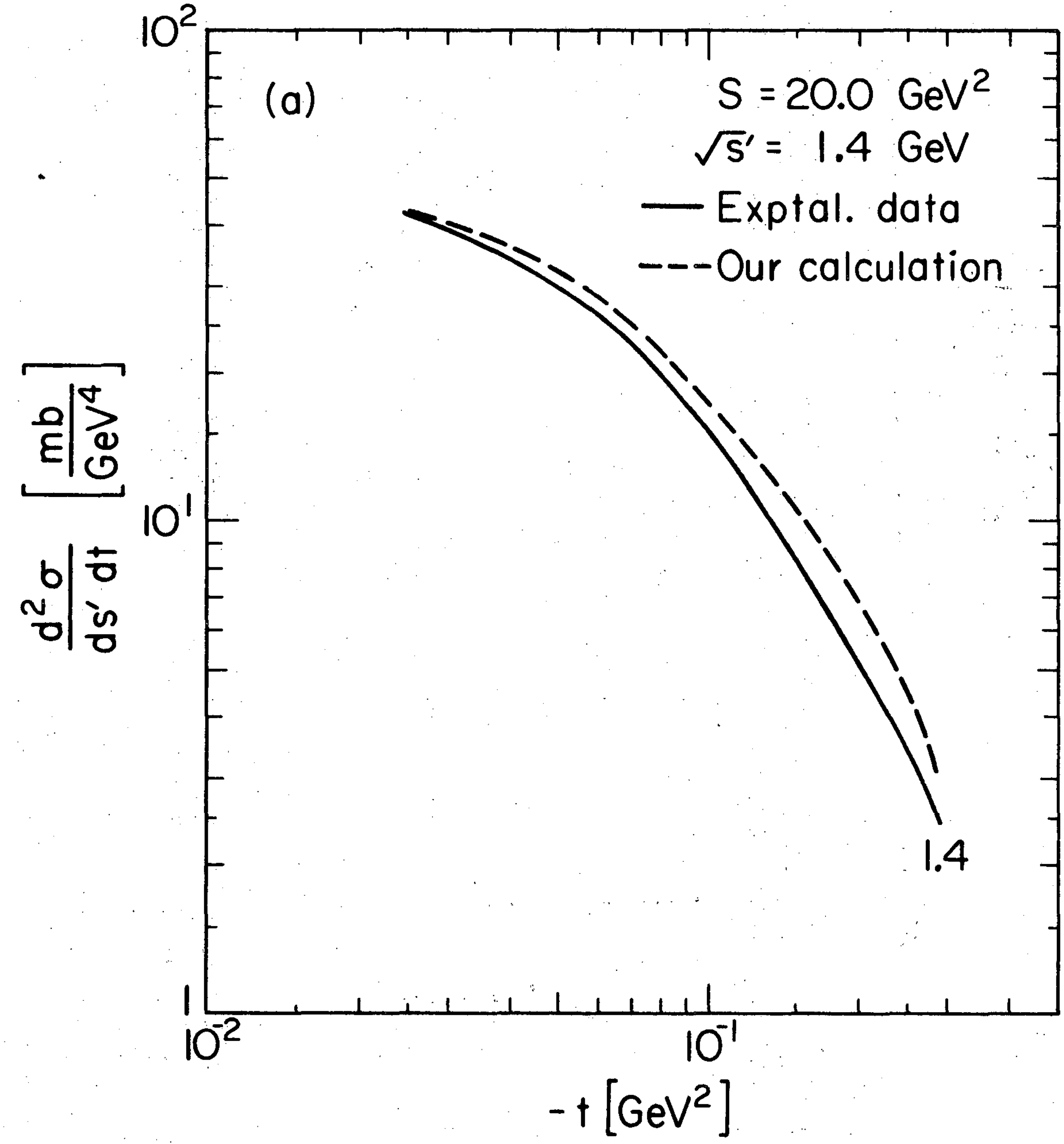

XBL724-2840

Fig. 5a

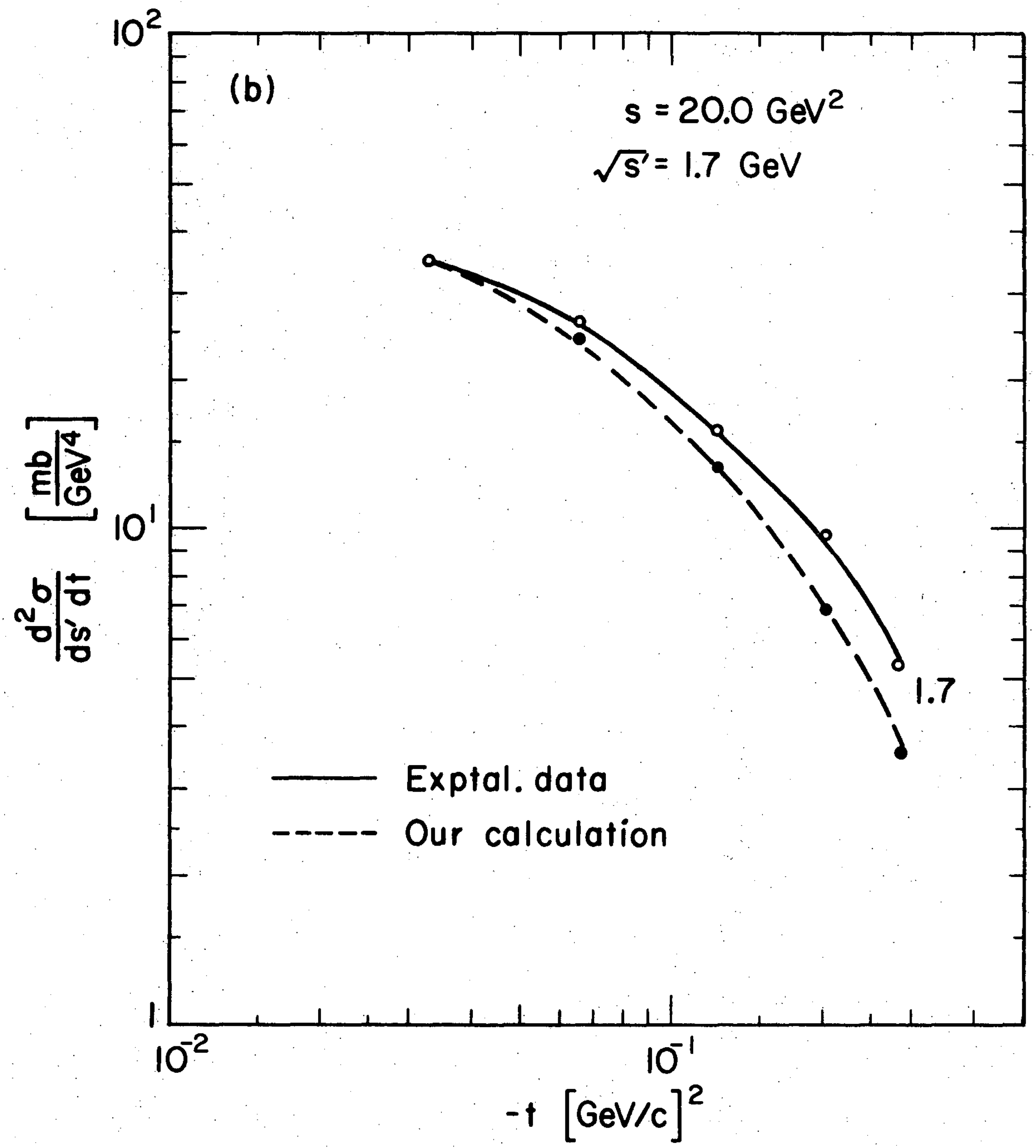

XBL 724-2841

Fig. 5b

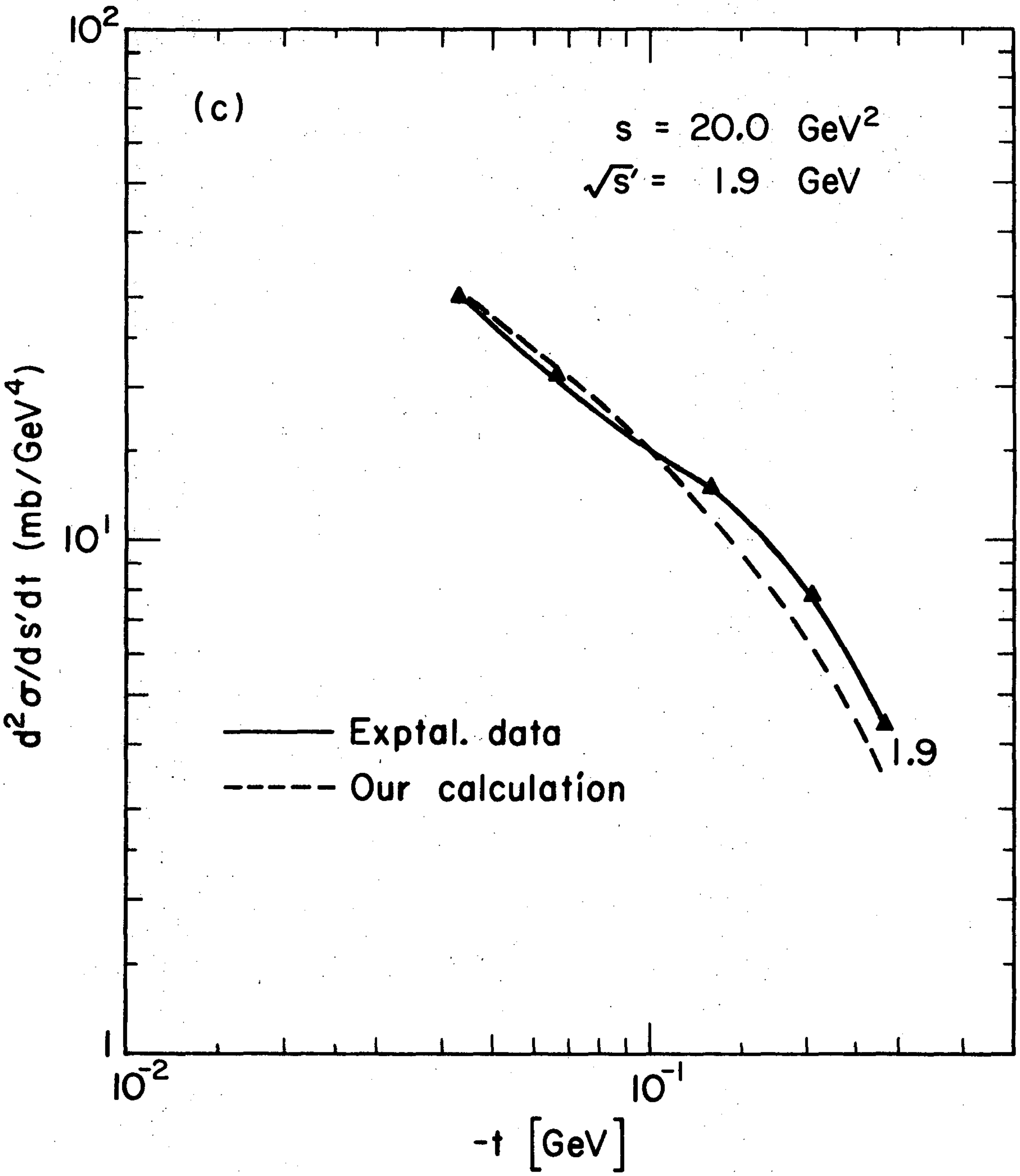

XBL724-2839

Fig. 5c

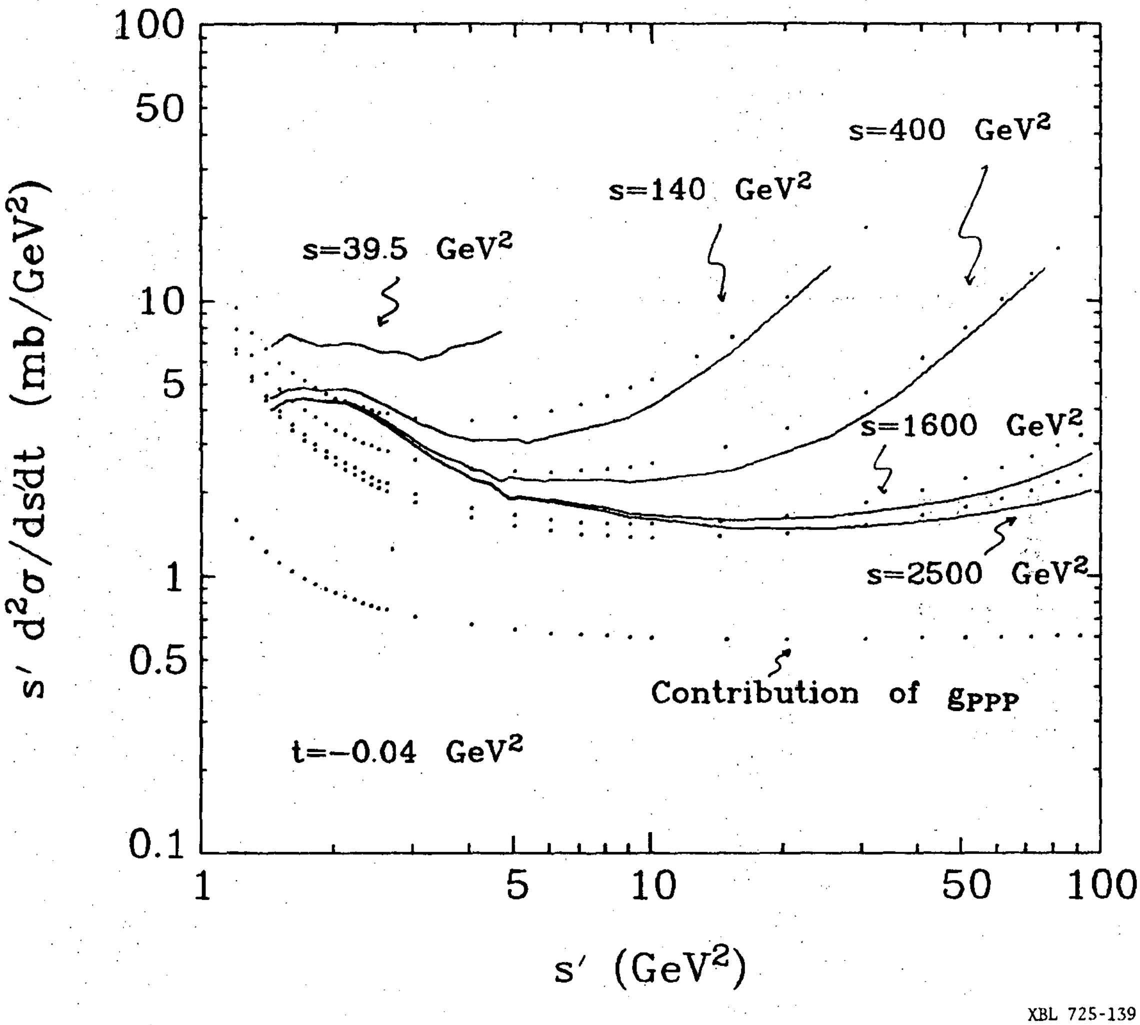
100
50
10
5
1
0.5
0.1
1
5
10
50
100
s' d²σ/ds'dt (mb/GeV²)
s' (GeV²)
s=39.5 GeV²
s=140 GeV²
s=400 GeV²
s=1600 GeV²
s=2500 GeV²
Contribution of gPPP
t=−0.04 GeV²
XBL 725-139

Fig. 6

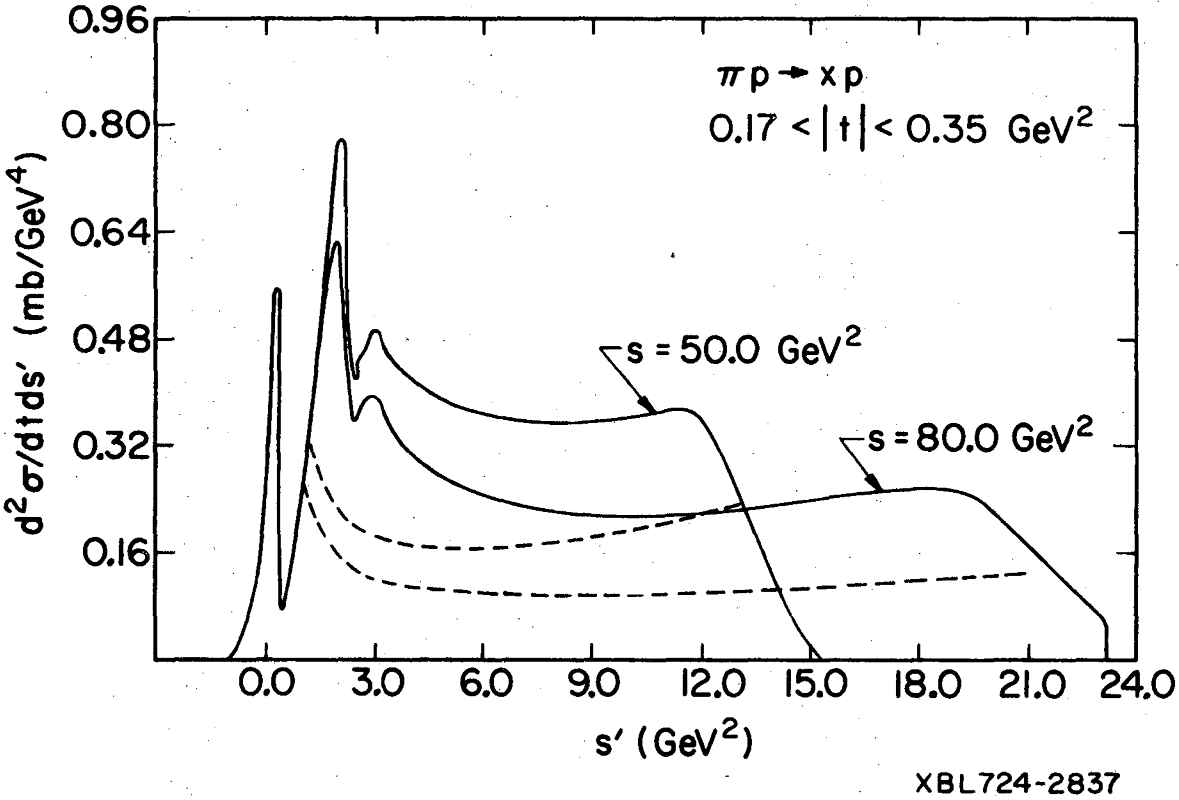

$\pi p \to x p$
$0.17 < |t| < 0.35$ GeV^2
s = 50.0 GeV^2
s = 80.0 GeV^2
$d^2\sigma/dt\,ds'$ (mb/GeV^4)
0.96
0.80
0.64
0.48
0.32
0.16
0.0
3.0
6.0
9.0
12.0
15.0
18.0
21.0
24.0
s' (GeV^2)
XBL724-2837

Fig. 7

TECHNICAL INFORMATION DIVISION
LAWRENCE BERKELEY LABORATORY
UNIVERSITY OF CALIFORNIA
BERKELEY, CALIFORNIA 94720